RSC Advances

PAPER

View Article Online
View Journal | View Issue

Cite this: *RSC Adv.*, 2022, **12**, 18215

Thiourea modified low molecular polyamide as a novel room temperature curing agent for epoxy resin

Zhiyong Huang, Huixin Zhu,* Guofeng Jin,* Yuanzheng Huang and Minna Gao

A thiourea modified low molecular weight polyamide (TLMPA) as a room temperature curing agent was synthesized by a two-step method. Firstly, a low molecular weight polyamide curing agent (LMPA) with low viscosity and high amine value was synthesized by amidation of sebacic acid with tetraethylenepentamine, then the synthesized curing agent was modified with thiourea to increase its reactivity at room temperature. The optimal reaction conditions were studied by $L_9(3^3)$ orthogonal experiments. The structure of the prepared curing agent was analyzed by Fourier transform infrared spectroscopy (FT-IR). The kinetics of TLMPA curing of E-51 epoxy resin was analyzed using the Kissinger method with non-isothermal differential scanning calorimetry (DSC). The activation energy of TLMPA/E-51 calculated by the Kissinger method and FWO method was 38.79 kJ mol^{-1} and 42.73 kJ mol^{-1}. The nano-SiO_2 filler was compounded with E-51 epoxy resin, TLMPA, allyl glycidyl ether diluent, and KH-560 coupling agent to prepare the room temperature curing epoxy resin (EP) system. $L_9(3^4)$ orthogonal experiments were carried out to study the effect of various factors on the mechanical properties of the cured resin systems. The best formulation of the system is that the content of nano-SiO_2, curing agent, diluent, and coupling agent is 3, 35, 15, 1 wt%, respectively. With the optimal formulation, the tensile and shear strength, tensile strength, impact strength, and bending strength of the cured EP system was 13.19 MPa, 53.8 MPa, 52.16 kJ m^{-2}, and 94.95 MPa, respectively.

Received 28th April 2022
Accepted 30th May 2022

DOI: 10.1039/d2ra02693g

rsc.li/rsc-advances

1. Introduction

Epoxy resin systems have the advantages of low curing shrinkage, good material compatibility, high bonding strength, and good corrosion resistance.[1–3] Commercial applications have included the most versatile multi-functional polymerization for more than half a century. However, EP itself has a chain-like thermoplastic structure, which has an application value only after cross-linking into a three-dimensional network structure under the action of a curing agent.[4] According to the classification of curing conditions, cold curing (including low temperature curing and room temperature curing), hot curing, and other curing methods (including UV curing, acoustic curing, *etc.*) are distinguished. Compared with other curing methods, room temperature curing (curing temperature 15–40 °C) has the advantages of low shrinkage caused by the thermal expansion difference, low internal stress, low energy consumption, and low toxicity. It is usually used in oilfield plugging, building structural repairs, cultural relics' restoration, and other occasions where heating curing is not allowed.[5] Aliphatic amines, modified aliphatic amines, and low molecular weight polyamines can be used as room temperature curing agents of EP among which low molecular weight polyamines and phenolic amines are the most commonly used room temperature curing agents of EP.[6]

The low molecular weight polyamide curing agent (LMPA) is generally formed by polycondensation of dimer acid and polyamine. Compared with other curing agents, the low molecular polyamide has low toxicity, good flexibility, strong adhesion, and other advantages. However, the low molecular weight polyamide synthesized from the dimer acid has low active hydrogen content and exhibits shortcomings such as low amine value, high viscosity, and low curing speed, which limit its application in casting and room temperature curing.[7–9] Compared with the traditional dimer acid, the low molecular polyamide prepared from a dibasic acid has a lower relative molecular mass, exhibits lower viscosity, and has higher active hydrogen and amide content per unit mass, showing higher reactivity. It also has a longer rotatable single bond molecular skeleton, showing better flexibility.[10,11] In order to speed up the curing reaction, thiourea can also be used to modify the amine curing agent or as a reinforcement accelerator.[12] At the same time, the introduction of –SH group can significantly increase the curing speed of amine curing agent, improve the brittleness of curing agent, and reduce its toxicity. Under certain reaction conditions, the highly electronegative N atom of the primary amine in the amine curing agent reacts with the C atom in the thiourea

Xi'an Institute of High Technology, Xi'an 710000, China. E-mail: zhuhx21@126.com

(H_2NCSNH_2) in a nucleophilic reaction, and the thiourea modified curing agent is obtained by removing NH_3 and condensation.[13] The reaction principle is as follows: Fig. 1.

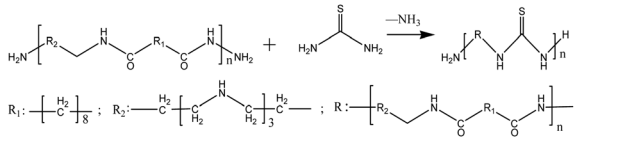

Fig. 1 Reaction formula for preparing thiourea modified hardener.

In order to improve the application and performance of EP, diluents are used to reduce the viscosity of the system after preparing the curing agent at room temperature. Fillers are used to increase the thermal conductivity of the system during curing to prevent detonation and improve mechanical properties. Coupling agents are used to improve the dispersion state and bonding performance of filler.[14] The performance of epoxy adhesive is affected by the interaction of various components. Therefore, it is necessary to use the orthogonal experiment method to optimize the multi-component design, and the trends can be analyzed by the average of the experimental results of each group at the same level of different factors in the orthogonal test.

In this study, the LMPA was initially synthesized and then the –SH group was introduced by modifying the structure of polyamide with a thiourea group. The physicochemical properties of LMPA before and after modification were characterized, and its curing kinetics was analyzed. Based on the modified curing agent, the EP system was formed by doping the KH-560 coupling agent, AGE diluent, and modified nano-SiO_2 filler. A room temperature curing EP system with good mechanical properties was constructed.

2. Experimental

2.1 Materials

Diglycidyl ether of bisphenol A DGEBA (commercial name: E51) was supplied by the Sinopec Corp. Baling Branch. Sebacic acid (≥99%) was obtained from Tianjin Fuchen Chemical Reagent Factory. Tetraethylenepentamine (≥99%) was purchased from Chengdu Kelon Chemical Reagent Factory. Thiourea (≥99%) was obtained from the fine chemical plant of Laiyang Economic and Technological Development Zone. Acetic acid (≥99%), benzene (≥99%), and ethanol (99.5%) were purchased from Xi'an Sanpu Chemical Reagent Co. Ltd. N_2 (99.999%) was acquired from Shaanxi Xinkang Medical Gas Co., Ltd. γ-(2,3-Epoxypropoxy) propyltrimethoxysilane (KH-560, ≥97%) was obtained from Jinan Xingchi Industry Co. Ltd. Nano-SiO_2 (average particle size 20 nm, content 99.5%) was purchased from Jiangsu Tianxing New Material Co. Ltd. Alkyl (C12–C14) glycidyl ether (AGE) was supplied by Guangzhou Yuebao Chemical Technology Co. Ltd.

Table 1 Orthogonal experiments for preparation of LMPA

Factors	Reaction time/h	Reaction temperature/°C	Ratio of raw materials
Level 1	1.5	160	2
Level 2	2	180	2.5
Level 3	2.5	200	3

2.2 Synthesis of curing agents

2.2.1 Synthesis of LMPA. An $L_9(3^3)$ orthogonal table was used to investigate the effects of reaction conditions on the viscosity and amine value of low molecular polyamide so as to determine the best reaction conditions for the preparation of LMPA. The factor levels are shown in Table 1.

The specific process was: the certain amount of sebacic acid was placed in a 250 mL three-necked flask equipped with magnetic stirring, a condenser, and a nitrogen-protection device and heated to 130 °C in an oil bath. At 130 °C, the sebacic acid began to dissolve. 50 mL of tetraethylenepentamine was added *via* a constant pressure dropping funnel, stirred at medium speed, and heated to 200 °C under N_2 protection. After the reaction for 2 h, the heating was stopped, and the generated water and excess of tetraethylenepentamine were removed by distillation under reduced pressure at 5 mm Hg for 30 min, and cooled to 40 °C for storage at room temperature to obtain LMPA. Finally, a pale-yellow transparent product was acquired.

2.2.2 Synthesis of TLMPA. 50 g LMPA and 4 g thiourea were added into a 250 mL three-necked flask equipped with magnetic stirring, tail gas treatment, and nitrogen protection. The oil bath was heated to 100 °C, stirred at medium speed, and the heating was stopped after 1 h of reaction. The small molecule ammonia gas was distilled off under reduced pressure, and the residue was cooled to 50 °C for storage to obtain TLMPA.

2.3 Preparation of EP system

In this study, the effects of various factors on curing speed and mechanical properties of room temperature cured EP system were investigated by orthogonal experiments. Four factors and three levels of KH-560 coupling agent (1, 3, 5 wt%), AGE diluent

Table 2 Levels of orthogonal experimental factors

	Factors			
Level	Dosage of coupling agent/wt% (A)	Dosage of diluent/wt% (B)	Dosage of filler/wt% (C)	Dosage of curing agent/wt% (D)
1	1	10	0	30
2	3	15	3	35
3	5	20	5	40

(10, 15, 20 wt%), modified nano-SiO_2 filler (0, 3, 5 wt%), and curing agent (30, 35, 40 wt%) were selected to design $L_9(3^4)$ orthogonal experiments, as shown in Table 2.

The specific process was: the certain amount of modified nano-SiO_2 was dissolved in acetone, and the nano-SiO_2 was evenly dispersed in acetone by ultrasonic treatment for 10 min. The acetone solution of nano-SiO_2 was added to E-51 epoxy resin, stirred evenly, and dispersed in E-51 by ultrasound at 70 °C for 2 h. After that, the acetone in the system was removed in water bath at 70 °C for 10 h. E-51/nano-SiO_2, AGE diluent, and KH-560 coupling agent were mixed according to the proportion and stirred evenly, and then vacuum degassing was performed. Finally, a certain proportion of curing agent was added and stirred evenly to obtain the EP system.

2.4 Characterization

The amine value of LMPA was determined by perchloric acid non-aqueous titration. Viscosity was measured with an NDJ-1S rotary viscometer. Infrared spectra were recorded with a Nexus FT-IR spectrometer. Curing kinetics of the TLMPA/E-51 systems (5.0–10.0 mg) was analyzed by the DSC method (SDT-Q600 TG-DSC Analyzer) at different heating rates of 5, 10, 15, 20 °C min^{-1} under N_2 atmosphere at a constant flow of 50 mL min^{-1}. Lap tensile shear strength and bending strength were measured on a SANS CMT 7204 microcomputer control electronic universal testing machine at a bending rate of 2 mm min^{-1} and stretching rate of 2 mm min^{-1}. The charpy impact strength of the samples was examined with a ZBC-50B Impact Tester. Five samples of each compound were measured, and the average values were recorded. The fracture surfaces of the impact samples were examined with a VEGA II XMU scanning electron microscope (SEM).

3. Results and discussion

3.1 Determination of the best reaction conditions

The value of amine groups and viscosity measured under various conditions are shown in Table 3, and range analysis is shown in Table 4 and Fig. 2. It can be seen from Fig. 2 that within each factor level, amine value increased first and then decreased with the increase of reaction time. This is because the reaction time was too short, and a large amount of tetraethylenepentamine was not involved in the reaction and was not steamed out. The reaction temperature had a little effect on the amine value. When the amount of amine increased, the condensation degree was lower, the content of free amine increased, the amine value increased, and the viscosity decreased. The viscosity increased with the increase of reaction time and decreased with the increase of reaction temperature. This is because the reaction time increased, the degree of condensation increased, the content of free amine decreased, and when the reaction temperature increased, part of the amide terminal rings was converted into imidazoline rings, reducing the viscosity of the system. It can be seen from Table 3 that the importance of each factor regarding viscosity and amine value is as follows: raw material ratio > reaction time > reaction temperature; raw material ratio > reaction temperature > reaction time. The optimal reaction conditions were as follows: reaction time 2 h, temperature 200 °C, ratio of amine to acid 3 when low viscosity and high amine value were used as indexes. Under these conditions, the value of LMPA was 745 mg KOH g^{-1} and the viscosity was 3.172 Pa s, which is consistent with the results of orthogonal experiments. According to the amine value, the theoretical dosage of LMPA was 33%. According to the ratio of E-51/LMPA, the gel time of EP adhesive measured at room temperature (25 °C) was 64 min, and the curing time was 173 min.

3.2 FTIR characterization

The LMPA synthesized under optimal reaction conditions was characterized by FTIR, and the results are shown in Fig. 3. It can be seen that the stretching vibration peak intensity of $-NH_2$ of LMPA at about 3280 cm^{-1} is lower than that of tetraethylenepentamine, indicating that the reaction consumes $-NH_2$ of tetraethylenepentamine. The stretching vibration peaks of C–N and C=O in the amide group are at 1460 cm^{-1} and 1650 cm^{-1}, respectively, and the bending vibration peak of N–H in the amide group is at 1560 cm^{-1}, indicating that the reaction product has a polyamide structure.[15,16]

When modifying LMPA, the amount of modifier, reaction temperature, and reaction time are the main factors affecting the properties of TLMPA. In Fig. 4, 1450 cm^{-1}, 1560 cm^{-1}, and 1650 cm^{-1} are characteristic peaks of amide groups. The absorption strength of TLMPA at the stretching vibration peak of $-NH_2$ at about 3280 cm^{-1} and the bending vibration peak of primary amine N–H at 760 cm^{-1} was obviously lower than that

Table 3 Orthogonal experimental results of preparation of low molecular polyamide

Factors	Reaction time/h	Reaction temperature/°C	Ratio of raw materials	Amine value/mg KOH g^{-1}	Viscosity/Pa s
Experiment 1	1.5	160	2	427	62.125
Experiment 2	1.5	180	2.5	592	6.265
Experiment 3	1.5	200	3	680	3.428
Experiment 4	2	160	2.5	676	16.700
Experiment 5	2	180	3	740	4.178
Experiment 6	2	200	2	595	50.371
Experiment 7	2.5	160	3	744	4.670
Experiment 8	2.5	180	2	493	73.120
Experiment 9	2.5	200	2.5	628	9.362

Table 4 Orthogonal experimental results of preparation of low molecular polyamide

Factors	Reaction time/h	Reaction temperature/°C	Ratio of raw materials
Mean amine values 1	566.33	615.67	505.00
Mean amine values 2	670.33	608.33	632.00
Mean amine values 3	621.67	634.33	721.33
Range of amine values	104.00	26.00	216.33
Average viscosity 1	23.936	27.831	61.872
Average viscosity 2	23.749	27.851	10.772
Average viscosity 3	29.050	21.053	4.092
Range of viscosities	5.301	6.797	57.780

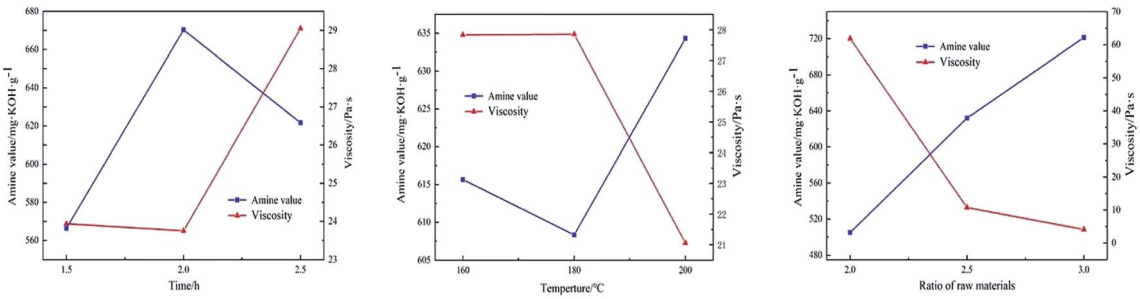

Fig. 2 Range analysis of influencing factors.

of LMPA because the deamination condensation reaction removed part of primary amine groups of LMPA. The characteristic absorption peak at 2050 cm^{-1} is C≡N, indicating that a small amount of NH_4SCN is generated by a side reaction.[17]

Fig. 5 shows the FTIR diagram before and after 6 h curing at 25 °C after mixing TLMPA and E-51. It can be seen from the figure that the characteristic peak of epoxy group (at 915 cm^{-1}) of the EP system corresponding to the synthetic curing agent completely disappeared after curing for 6 h, indicating that the curing degree was relatively complete.[18]

It is worth noting that after curing the E-51/TLMPA mixture, no characteristic peak was found at 2500–2600 cm^{-1}, the common spectrum segment of the –SH group.[19] The strength of –SH group itself is weak and difficult to detect also due to the interference of conjugated double bonds or triple bonds in the system.[20] At the same time, because LMPA itself is a kind of polymer and its specific molecular weight is difficult to measure, the modified TLMPA is a mixture, so it is difficult to measure the probability of the occurrence of –SH group in the curing process. As can be seen from the references,[21–24] the nucleophilic reaction between the C atom in thiourea and the N atom with strong electronegativity in the primary amine is relatively complete in the oil bath heating environment. At the same time, because thiourea itself is a solid, if the reaction had not been completed, the mechanical properties of E-51/TLMPA would have been reduced, but such a situation was not found in the test, so the modification of thiourea was relatively complete.

3.3 Curing kinetics of TLMPA

The DSC curve of E-51/TLMPA system is shown in Fig. 6. As can be seen from the figure, there is only one peak in the curing process of TLMPA, indicating that the prepared hardener has good compatibility with E-51.

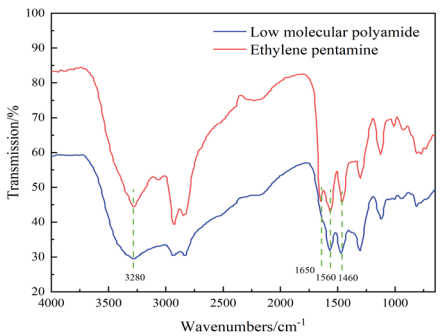

Fig. 3 FTIR diagram of ethylene pentaamine and low molecular polyamide.

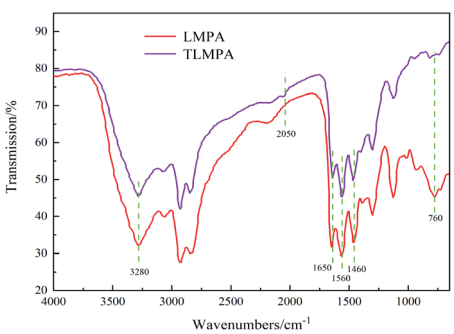

Fig. 4 FTIR diagram of thiourea modified hardener.

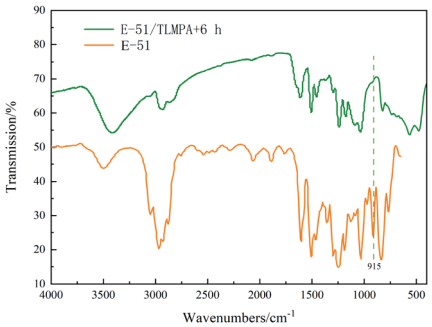

Fig. 5 FTIR diagram after curing at 25 °C for 6 h.

The Kissinger equation is as follows:[25–27]

$$-\ln\left(\frac{\beta}{T_p^2}\right) = \frac{E_a}{RT_p} - \ln\frac{AR}{E_a}$$

where β is the heating rate, T_p is the peak exothermic temperature of DSC curve, R is the ideal gas constant, and A is the Arrhenius constant.

The linear fitting diagram of $\ln(\beta/T_p^2)$ and $1/(R \times T_p)$ is shown in Fig. 7. The regression coefficient of the fitting line is 0.9924, indicating that the Kissinger equation fits well. E_a and A can be obtained by combining its slope a_1 and intercept B. If $E_a = a_1$, $A = E_a \times \exp(-b)/R$, the rate constant $k = A \times \exp(-E_a/RT)$ can be calculated by the Arrhenius equation. From the slope 38.795 and intercept −3.032, the apparent activation energy E_a is 38.795 kJ mol^{-1}, Arrhenius constant $A = 9.68 \times 10^4$, and the reaction rate constant $K = 0.0154$ at 25 °C.

The Flynn–Wall–Ozawa equation is as follows:

$$\ln\beta = \ln\left(\frac{AE_a}{R}\right) - \ln f(\alpha) - 5.331 - 1.052\left(\frac{E_a}{RE_a}\right)$$

Table 5 shows the characteristic temperature values of the system at different heating rates, according to which the linear fitting diagram of $\ln\beta$ and $1/T_p$ is shown in Fig. 8. It can be seen from Fig. 8 that the regression coefficient of the fitting line is 0.9997, indicating that the Flynn–Wall–Ozawa equation is accurately fitted. From its slope a_2, the activation energy $E_a = -R \times a_2/1.052 = 42.73$ kJ mol^{-1}.

The Crane method to calculate the reaction order n:

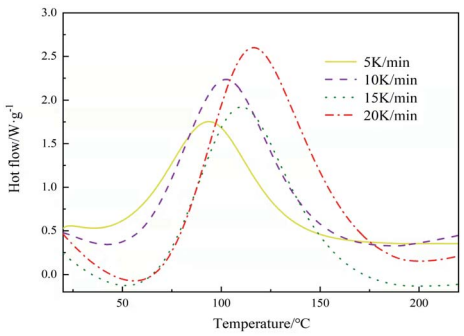

Fig. 6 DSC curves of modified hardener at different heating rates.

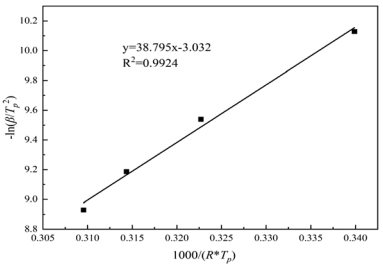

Fig. 7 Linear fitting of $\ln(\beta/T_p^2)$ and $1/(R \times T_p)$ modified hardener.

$$\frac{d(\ln\beta)}{d(1/T_p)} = -\frac{E_a}{nR} - 2T_p$$

where E_a is the activation energy of reaction obtained by the Kissinger method. When E_a is far greater than $2T_p$, the formula simplifies to calculate n, $n = -E_a/(K \times R) = 0.86$, which indicates that the curing process of E-51/TLMPA is a complex multistage reaction.

The T–β extrapolation method was used to study the gel temperature, curing temperature, and post-curing temperature of the curing system when β was zero. The T–β fitting diagram is shown in Fig. 9. It can be seen from the figure that the linear fitting degree between the three characteristic temperatures and the heating rate is high (R_2 is greater than 0.92). When β is zero, the T_i, T_p, and T_f of the curing system are 37.10, 72.81, and 108.77 °C, respectively, indicating that the curing agent synthesized meets the requirements of room temperature curing.

3.4 Performance of EP system

Mechanical properties and gel time of each group in orthogonal tests are shown in Table 6.

Table 5 Characteristic temperature values of TLMPA systems at different heating rates

Heating rate/(K min^{-1})	T_i/°C	T_p/°C	T_f/°C	T_p/K
5	43.1	80.72	121.35	353.87
10	58.1	99.58	145.75	372.73
15	66.93	109.46	158.67	382.61
20	70.1	115.41	170.91	388.56

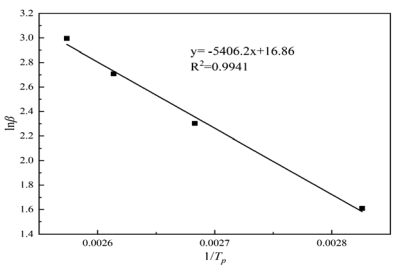

Fig. 8 Linear fitting of $\ln\beta$ and $1/T_p$.

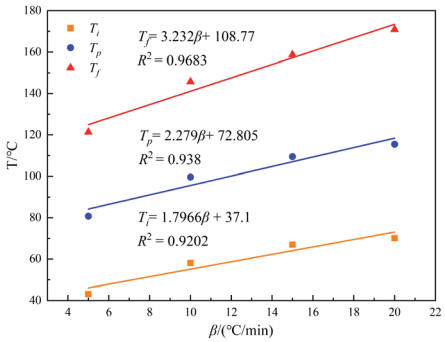

Fig. 9 Linear fitting diagram of modified curing agent $T-\beta$.

3.4.1 Tensile and shear strength. Table 7 shows the mean values of tensile and shear strength at different levels of each factor. Tensile and shear strength is an important index indicating whether the EP system can form a firm connection with the surface to be bonded. It can be seen from Table 7 that the important factors influencing the tensile and shear strength of EP are as follows: filler > coupling agent > curing agent > diluent, and the optimal combination for tensile and shear strength is A2B3C2D2. With the increase of filler, the tensile shear strength increased first and then decreased slightly. When the added amount was 3 wt%, the tensile shear strength reached the maximum, which was 47.12% higher than that without the nano-filler. This is because with the addition of nano-SiO_2, the curing shrinkage rate was reduced and the residual stress in the adhesive layer was reduced. When the adhesive layer is subjected to tensile shear stress, the evenly dispersed nanoparticles in the adhesive layer can absorb part of the stress and improve the shear strength. When it exceeds 3 wt%, the probability of collision and agglomeration between particles increases, and the reunited particles cause an increase in stress concentration points, resulting in a decrease in tensile and shear strength.[28] With the increase of dosage of coupling agent, the shear strength increased slightly, this is because the coupling agent has polar and nonpolar groups. The nonpolar groups tend to chemical combination with the epoxy system, rather than the polar groups can react with the surface of the metal. –OH generated help improve the ether bond, and when its content was more than 3 wt%, the enhancement effect was not obvious.

Table 7 Average analysis of tensile and shear strength of all factors

Factors	A	B	C	D
Mean 1	10.96	11.18	9.07	11.49
Mean 2	11.93	11.51	13.35	12.05
Mean 3	11.80	11.99	12.26	11.14
Range	0.97	0.81	4.28	0.91

3.4.2 Impact strength. Table 8 shows the mean value analysis of impact strength at different levels of various factors. Impact strength is an important index indicating toughness of EP system. It can be seen from Table 8 that the influence of each factor on impact strength is in the order of filler > curing agent > diluent > coupling agent, and the optimal combination for impact strength is A2B2C2D3. The impact strength increased firstly and then decreased with the increase of filler. The impact strength reached the maximum when the added amount was 3 wt%, which was 67.27% higher than that without the nano-filler. The main reason is that when the casting with the nano-SiO_2 filler is impacted, the nanoparticles and the EP bonded to them are transformed into silver cracks, absorbing and converting part of the impact energy. However, when the dosage was further increased, more serious particle agglomeration was caused, and the particle size of the agglomeration became larger, and the bonding force of the agglomeration with the EP system decreased. When subjected to impact force, these agglomeration particles became the stress concentration point, which is prone to producing large cracks, and then the impact strength decreased to some extent.[29] The impact strength increased with the increase of curing agent. This is because the

Table 8 Average impact strength analysis for all factors

Factors	A	B	C	D
Mean 1	37.44	39.67	29.83	36.47
Mean 2	40.34	42.46	49.90	40.44
Mean 3	40.30	38.58	40.98	43.79
Range	2.90	3.88	20.07	7.32

Table 6 Orthogonal experiment and test results

	Factors							
Group	A	B	C	D	Shear strength/MPa	Impact strength/kJ m^{-2}	Tensile strength/MPa	Bending strength/MPa	Gel time/min
1	1	1	1	1	8.01	25.33	30.25	74.18	28
2	1	2	2	2	13.19	52.16	53.8	94.95	24
3	1	3	3	3	11.67	34.84	46.61	91.18	24
4	2	1	3	2	12.74	40.72	43.12	89.15	23
5	2	2	1	3	8.97	35.71	34.7	82.04	22
6	2	3	2	1	14.08	44.58	52.19	93.38	31
7	3	1	2	3	12.79	52.95	46.46	93.41	20
8	3	2	3	1	12.38	39.5	48.08	87.56	27
9	3	3	1	2	10.23	28.44	35.44	83.92	26

synthesized curing agent itself is flexible with a long straight chain. In the scope of investigation of the amount of curing agent, the increase of the amount caused the enhancement of impact toughness.

3.4.3 Tensile strength. Table 9 shows the mean value analysis of tensile strength at different levels of various factors. It can be seen from Table 8 that the influence degree of each factor on tensile strength is filler > diluent > curing agent > coupling agent, and the optimal combination for tensile strength is A1B2C2D2. With the addition of nano-SiO_2, the tensile strength of epoxy casting increased significantly. When the content was 3 wt%, the tensile strength increased by 51.82%. Nano-SiO_2 is connected to EP through Si–O bonds, and the Si–O bond energy (460 kJ mol^{-1}) is higher than the C–C bond (332 kJ mol^{-1}) and C–O bond (326 kJ mol^{-1}), so they can absorb more energy when a fracture occurs.[30] As the content continued to increase, the collision frequency between particles increased, leading to agglomeration of nanoparticles more easily, thus forming a stress concentration point, resulting in a decline in tensile strength. With the addition of diluent, the tensile strength increased first and then decreased slightly because the addition of diluent significantly reduced the viscosity of EP system, effectively avoided the introduction of bubbles in the sample during the preparation, and rigid nanoparticles could be evenly dispersed in the system, thus improving the tensile strength. However, as the AGE diluent is a long-chain aliphatic monoepoxy compound of C12–C14, which does not contain rigid benzene ring structure, the curing crosslinking density decreased with the increase of dosage, resulting in a decrease in tensile strength.

3.4.4 Bending strength. Table 10 shows the mean value analysis of bending strength at different levels of various factors. Bending strength is an important index indicating the flexibility of epoxy casting. According to Table 10, the influence degree of each factor on bending strength is in the order of filler > curing agent > diluent > coupling agent, and the optimal combination for bending strength is A3B3C2D2. Appropriate addition of nano-SiO_2 can effectively improve the bending strength of the cast, indicating that nano-SiO_2 can improve the flexibility of the cast. Nano-SiO_2 modified by the coupling agent has an elastic three-dimensional network structure. The Si–O bond (0.164 nm) is longer than the C–C bond (0.154 nm) and C–O bond (0.143 nm), so it is pliant. Moreover, the addition of rigid nanoparticles makes the casting subjected to bending stress produce silver strike cracks so as to absorb and transform part of the energy. The bending strength increased by 17.33%. With the increase of the amount of nano-filler, the collision and agglomeration of particles inevitably accelerate. Due to the larger particle size, the effective bonding degree of nanoparticles with the cast decreased, which is more likely to cause stress concentration and destructive cracks when subjected to external forces, resulting in the decrease of the bending strength of the cast.

3.4.5 Impact section morphology analysis. In the above analyses, the amounts of filler and curing agent are the main reasons affecting the impact performance of the casting. In order to investigate the influence of different dosages of nano-SiO_2 on the impact section of casting body, the content of curing agent 9, 2, and 4 was 35 wt% and nano-SiO_2 was 0, 3, and 5 wt%, respectively, and the impact section was analyzed by SEM, as shown in Fig. 10.

As can be seen from the SEM figure, the intersection of light and shade of the three groups of fracture sections indicates that the section is uneven and rough, and the cracks have many branches and obvious fish scales and ripples, which are typical ductile fracture characteristics. When the amount of nanoparticles was 0 wt%, the dimple content in the section was the least. When the amount of nanoparticles was 3 wt%, the dimple content in the section was the highest, and the distribution of the river line direction of the fracture was more divergent, indicating that the addition of nano-SiO_2 can effectively absorb part of the impact energy and interrupt or change the crack

Table 9 Analysis of average tensile strength for all factors

Factors	A	B	C	D
Mean 1	43.55	39.94	33.46	43.51
Mean 2	43.34	45.53	50.82	44.12
Mean 3	43.33	44.75	45.94	42.59
Range	0.23	5.58	17.35	1.53

Table 10 Analysis of average bending strength for factors

Factors	A	B	C	D
Mean 1	86.77	85.58	80.05	85.04
Mean 2	88.19	88.18	93.91	89.34
Mean 3	88.30	89.49	89.30	88.88
Range	1.53	3.91	13.87	4.30

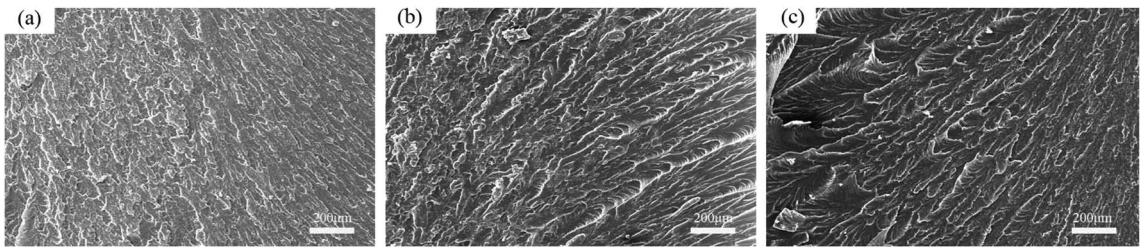

Fig. 10 SEM of impact section (a) 0 wt% (b) 3 wt% (c) 5 wt%.

growth, and the corresponding impact strength was the highest. When the amount of nanoparticles was 5 wt%, the dimple content was less than 3 wt% but more than 0 wt%, and it is obvious that there are some secondary agglomerated nanoparticles on the surface, which are relatively loosely bonded with the epoxy system.[31]

3.4.6 Comprehensive balance method to determine the optimal ratio. According to the orthogonal test results, the influence degree of each factor on the mechanical properties and heat resistance of epoxy tree system is as follows: tensile and shear strength C > A > D > B, impact strength C > D > B > A, tensile strength C > B > D > A, bending strength C > B > D > A. The optimal combination is A2B3C2D2 with the maximum tensile strength index, A2B2C2D3 with the maximum impact strength index, A1B2C2D2 with the maximum tensile strength index, and A3B3C2D2 with the maximum bending strength index. The optimal ratio for different performance is different, so the comprehensive balance method was used to determine the optimal ratio.[32]

The amount of filler is the primary factor affecting mechanical properties and heat resistance. For mechanical properties, C2 is the best, while for heat resistance, C3 is the best. But improving mechanical properties is the main purpose of this paper, so the level was determined as C2. The amount of diluent is the second factor affecting the impact and bending strength, the third factor affecting the impact strength, and the fourth factor affecting the tensile and shear strength. For the impact and tensile strength, B2 is the best. For tensile, shear, and bending strength, B3 is the best. In order to give consideration to the performance and the actual use, this level was determined as B2. The amount of curing agent is the second factor affecting the bending and impact strength and the third factor affecting the tensile, shear and tensile strength. For the tensile, shear, and bending strength, D2 is the best. For impact strength, D3 is optimal. All things considered, this level was determined to be D2. The amount of coupling agent has a little effect on the casting properties, and A1 is the best for tensile properties. For tensile, shear, and impact strength, A2 is the best. For bending strength, A3 is the best. Considering application cost, this level is A1. Therefore, the optimal ratio was determined as A1B2C2D2 (ratio no. 2). In this case, the corresponding tensile and shear strength was 13.19 MPa, tensile strength was 53.8 MPa, impact strength was 52.16 kJ m^{-2}, bending strength was 94.95 MPa, and T_{max} was 371.98 °C, indicating good comprehensive performance.[33]

4. Conclusions

In conclusion, a TLMPA was synthesized by a two-step method. After that, the optimal formulation of the room temperature curing EP system was 3, 35, 15, and 1 wt% of nano-SiO_2, curing agent, diluent, and coupling agent, respectively. The tensile and shear strength was 13.19 MPa, the tensile strength was 53.8 MPa, the impact strength was 52.16 kJ m^{-2}, and the bending strength was 94.95 MPa. It provides a good idea for preparing a room temperature curing agent for EP and its application.

Author contributions

Zhiyong Huang: in this research activity, his main contributions are visualization, conceptualization and project administration. Huixin Zhu: in this research activity, his main contributions are methodology, formal analysis and writing – original draft. Guofeng Jin: in this research activity, his main contributions are supervision, funding acquisition and writing – review & editing. Yuanzheng Huanga: in this research activity, his main contributions are data curation, resources and software. Minna Gao: in this research activity, her main contributions are investigation and validation.

Conflicts of interest

All the authors declare no conflict of interest.

Acknowledgements

This work is supported by the Natural Science Foundation of Shaanxi Province of China (No. 2022JM-243).

References

1 D. Liu, D. Wang, Z. Li, Z. Li, X. Peng, C. Liu, Y. Zhang and P. Zheng, *Materials*, 2020, **13**, 2145–2184.
2 J. Kúdelčík, E. Jahoda and J. Kurimský, *Eur. Phys. J. Appl. Phys.*, 2019, **85**, 10401–10409.
3 Y. Xu, C. Chen, W. Rao, M. Qi, D. Guo, W. Liao and Y. Wang, *Chem. Eng. J.*, 2018, **347**, 223–232.
4 Z. Shao, Z. Tang, X. Lin, J. Jin, Z. Li and C. Deng, *Mater. Des.*, 2020, **187**, 108417–108428.
5 C. Jie, C. Na, Z. Miao, J. Fan and S. Park, *J. Appl. Polym. Sci.*, 2020, **137**, 49592–49612.
6 Y. Xu, A. Dayo, J. Wang, A. Wang, D. Lv, A. Zegaoui, M. Derradji and W. Liu, *Mater. Chem. Phys.*, 2018, **203**, 293–301.
7 A. Rudawska, *J. Adhes.*, 2019, **96**, 402–422.
8 Y. Lu, C. Li and Y. Wu, *J. Polym. Res.*, 2021, **28**, 68–80.
9 A. Rudawska, I. Haniecka, M. Jaszek and D. Stefaniuk, *Polymers*, 2018, **10**, 344–357.
10 D. Arati, T. Asiya, G. Shivaji, T. Aslam, T. Mohaseen and M. Noormahamad, *J. Appl. Polym. Sci.*, 2022, **139**, 52221–52232.
11 M. Zahra, S. Zulfiqar, W. Skene and M. Sarwar, *Polym. Int.*, 2019, **69**, 50–60.
12 B. Zhu, C. Zuo, X. Lin and J. Jin, *Mater. Des.*, 2020, **187**, 108417–108428.
13 G. You, H. He, B. Feng, Y. Tang, Z. Cheng and F. Fan, *Chem. Zvesti*, 2020, **74**, 2403–2414.
14 Y. Zhao, X. Zeng and W. Zhang, *Adv. Mater. Res.*, 2013, **652–654**, 127–130.
15 B. Liang, J. Wang, J. Hu, C. Li, R. Li, Y. Liu, K. Zeng and G. Yang, *Polym. Degrad. Stab.*, 2019, **169**, 108954–108962.
16 B. A. Kash, M. Aaron, M. Kennedy, W. Richard, G. Marianne and C. Patrice, *Polym. Chem.*, 2021, **12**, 1487–1497.

17 P. Ramesh, L. Ravikumar and A. Burkanudeen, *J. Therm. Anal. Calorim.*, 2013, **115**, 713–722.
18 Y. Li, Z. Zhou, X. Xu and L. Xie, *Adv. Mater. Res.*, 2013, **634–638**, 3008–3016.
19 N. B. Cramer and C. N. Bowman, *J. Polym. Sci. 1 Polym. Chem.*, 2001, **39**, 3311–3319.
20 T. M. Roper, C. A. Guymon, E. S. Jonsson and C. E. Hoyle, *J. Polym. Sci. 1 Polym. Chem.*, 2004, **42**, 6283–6298.
21 V. C. Rufino and J. R. Pliego, *Asian J. Org. Chem.*, 2021, **10**, 1–15.
22 O. V. Serdyuk, C. M. Heckel and S. B. Tsogoeva, *Org. Biomol. Chem.*, 2013, **11**, 7051–7071.
23 F. E. Held and S. B. Tsogoeva, *Catal. Sci. Technol.*, 2016, **6**, 645–667.
24 Y. J. Li, Z. G. Zang, K. Ji, P. Q. Ji, W. G. Ding and J. Liu, *Acta Chim. Sin.*, 2007, **9**, 834–840.
25 F. Yeasmin, A. Mallik, A. Chisty, F. Robel, M. Shahruzzaman, P. Haque, M. Rahman, N. Hano, M. Takafuji and H. Ihara, *Heliyon*, 2021, **7**, e05959.
26 B. L. Roger and H. Kissinger, *Thermochim. Acta*, 2012, **540**, 1–6.
27 L. Liu, S. Gao, Z. Jiang, Y. Zhang, D. Gui and S. Zhang, *Ind. Eng. Chem. Res.*, 2019, **58**, 14088–14097.
28 X. Li, G. Li and X. Su, *J. Polym. Eng.*, 2018, **39**, 10–15.
29 J. Zheng, X. Zhang, J. Cao, R. Chen, T. Aziz, H. Fan and C. Bittencourt, *J. Appl. Polym. Sci.*, 2020, **138**, 50138–50149.
30 H. Li, Z. Zhang, X. Ma, M. Hu, X. Wang and P. Fan, *Surf. Coat. Technol.*, 2007, **201**, 5269–5272.
31 C. Xiao, Y. Tan, X. Yang, T. Xu, L. Wang and Z. Qi, *Chem. Phys. Lett.*, 2018, **695**, 34–43.
32 A. Andrea, R. Katharina, M. A. Raj and W. Günter, *Macromol. Mater. Eng.*, 2019, **304**, 1900031–1900040.
33 X. Fan, J. Miao, L. Yuan, Q. Guan, A. Gu and G. Liang, *Appl. Surf. Sci.*, 2018, **447**, 315–324.